Journal of Materials Science and Chemical Engineering, 2024, 12, 29-48
https://www.scirp.org/journal/msce
ISSN Online: 2327-6053
ISSN Print: 2327-6045

Modification of Nano-α-Al_2O_3 and Its Influence on the Surface Properties of Waterborne Polyurethane Resin Composite Passivation Films

Jiankang Fu[1], Changshuai Ma[1], Yameng Zhu[1], Jing Yuan[2,3*], Qianfeng Zhang[1*]

[1]Institute of Molecular Engineering and Applied Chemistry, Anhui University of Technology, Ma'anshan, China
[2]Department of Civil Engineering, Tongling University, Tongling, China
[3]Department of Civil Engineering, Manitoba University, Winnipeg, MB, Canada
Email: *154427@tlu.edu.cn, *zhangqf@ahut.edu.cn

How to cite this paper: Fu, J.K., Ma, C.S., Zhu, Y.M., Yuan, J. and Zhang, Q.F. (2024) Modification of Nano-α-Al_2O_3 and Its Influence on the Surface Properties of Waterborne Polyurethane Resin Composite Passivation Films. *Journal of Materials Science and Chemical Engineering*, **12**, 29-48.
https://doi.org/10.4236/msce.2024.125003

Received: April 9, 2024
Accepted: May 27, 2024
Published: May 30, 2024

Abstract

Silane coupling agent KH560 was used to modify the surface of nano-α-Al_2O_3 in ethanol-aqueous solution with different proportions. The particle size of nano-α-Al_2O_3 was determined by nano-particle size analyzer, and the effects of nano-α-Al_2O_3 content, ethanol-aqueous solution ratio and KH560 dosage on the dispersion and particle size of nano-α-Al_2O_3 were investigated. The material structure before and after modification was determined by Fourier transform infrared spectroscopy (FTIR). Aqueous polyurethane resin and inorganic components are combined with modified nano-α-Al_2O_3 dispersion to form chromium-free passivation solution. The solution is coated on the galvanized sheet, the adhesion and surface hardness are tested, the bonding strength of the coating and the surface hardness of the substrate are discussed. The corrosion resistance and surface morphology of the matrix were investigated by electrochemical test, neutral salt spray test and scanning electron microscope test. The chromium-free passivation film formed after the modification of nano-α-Al_2O_3 increases the surface hardness of galvanized sheet by about 85%. The corrosion resistance of the film is better than that of a single polyurethane film. The results show that the surface hardness and corrosion resistance of polyurethane resin composite passivation film are significantly improved by the introduction of nano-α-Al_2O_3.

Keywords

Micro-Nano α-Al_2O_3, Waterborne Polyurethane Resin, Particle Size, Surface Hardness, Corrosion Resistance

*Corresponding authors.

1. Introduction

With the rapid progress of modern industrialization and technological development, surface coating technology plays an increasingly important role in the field of metal protection and functional improvement [1]. As a common metal substrate, galvanized sheet has been widely used because of its excellent corrosion resistance and good mechanical properties, and occupies an important position in the fields of construction, automobile manufacturing, energy and infrastructure construction [2]. At present, the methods to enhance the surface performance of galvanized sheet mainly include: surface coating technology, the coating of polymer, ceramic or other special materials can improve the corrosion resistance and wear resistance of galvanized sheet; The mechanical properties and corrosion resistance of galvanized sheet can be improved by adjusting the ratio of alloying elements or adding trace elements. Surface treatment technology, using chemical treatment, mechanical treatment or electrochemical treatment methods, improve the surface finish and roughness of galvanized sheet, improve its coating adhesion and corrosion resistance; Nanotechnology applications, the use of nanomaterials or nanostructures to modify galvanized sheets to improve their surface properties, such as enhancing hardness, corrosion resistance and wear resistance. These methods are usually used in combination to achieve a comprehensive improvement in the surface properties of galvanized sheets.

However, with the continuous changes in application environments and increasing usage requirements, there is an urgent need to significantly enhance the surface performance of galvanized steel [3] [4] [5]. This article aims to introduce new coating materials and modification methods to achieve substantial improvements in coating adhesion, corrosion resistance, and surface hardness of galvanized steel. At present, although the traditional chromium coating has a good application effect, the hexavalent and trivalent chromium ions contained in it have greater damage to the human body and the environment and have been gradually banned [6] [7]. The traditional anti-corrosion coating without chromium ion has been difficult to meet the complex and changing engineering needs.

Waterborne polyurethane is an environmentally friendly material that does not contain organic solvents and volatile organic compounds (VOCs), thus causing no pollution to the environment. Additionally, it possesses excellent physical and chemical properties, including high strength, abrasion resistance, chemical corrosion resistance, acid and alkali resistance, and good toughness, enabling it to withstand various complex application environments. Furthermore, waterborne polyurethane exhibits excellent adhesion and good affinity to various substrates, allowing it to form strong bonds with multiple base materials [8] [9].

However, the performance of a single water-based polyurethane resin in coatings still needs improvement, limiting its application in some high-demand

areas. To address this issue, it has been found through current research hotspots in metal surface coatings both domestically and internationally that selecting appropriate additives to enhance various properties of coatings is a new development direction.

Nano α-Al_2O_3, as an excellent nanomaterial [10], is an ideal choice for modifying waterborne polyurethane resin due to its superior physical and chemical properties. The α-Al_2O_3 particles possess a large specific surface area and extremely high hardness [11], enabling them to be uniformly dispersed within the coating, forming a hard, wear-resistant protective layer that effectively enhances the coating's hardness. Additionally, α-Al_2O_3 exhibits excellent chemical stability and corrosion resistance [12] [13]. By introducing it into the passivation solution, a dense protective film formed on the substrate surface can effectively isolate the metal surface from direct contact with corrosive factors in the environment. This film can also resist corrosion and degradation of the coating in harsh environments, providing reliable protection for the metal surface and enhancing the coating's corrosion resistance. The significance of this study lies not only in expanding the application of waterborne polyurethane resin in the field of metal coatings but also in providing new ideas and methods for improving coating performance. Furthermore, further exploration of the potential advantages of nan-α-Al_2O_3 modified waterborne polyurethane resin coatings in enhancing the surface properties of galvanized sheets and other related aspects will be conducted. This will provide more reliable protection measures for the application of metal materials in different environments, promoting the continuous and in-depth development of coating technology.

2. Experiments

2.1. Experimental Substrate Pretreatment

The experimental substrate selected is galvanized steel produced by Ma'anshan Iron & Steel Company Limited, with dimensions of 50 mm × 30 mm × 0.6 mm. The thickness of the zinc coating is 0.08 mm, and the roughness is 0.8 to 1.2 μm. The pretreatment process for the substrate includes the following steps: firstly, degreasing the substrate by immersing the samples completely in acetone or anhydrous ethanol, then cleaning with ultrasonic agitation for 30 minutes followed by rinsing with deionized water. Secondly, alkaline washing is conducted by immersing the sheet in a pre-configured alkaline solution, subjecting it to ultrasonic treatment for 40 minutes at room temperature (20˚C - 24˚C), the composition of the alkaline solution is 30 g/L $NaSiO_3$ and 10 g/L NaOH, followed by rinsing with water and drying. Lastly, the treated samples are placed in an oven at 90˚C for 40 seconds for drying.

2.2. Preparation of Nanometer α-Al_2O_3

In this paper, nano-α-Al_2O_3 powder particles were prepared by hydrothermal method [14] [15] [16]. The specific preparation process is described as follows:

The pure $Al_2(SO_4)_3$ powder was analyzed and dissolved in deionized water to form 1 mol/L $Al_2(SO_4)_3$. Mechanical stirring 60 min, filter to remove insoluble impurities in the solution. The concentration of 25% - 29% of ammonia water is dropped into the aluminum sulfate solution, at this time there will be white flocculent precipitate continuously, until the pH of 8 - 9 white suspension stop dripping. The white suspension is encapsulated in a high-pressure container for hydrothermal reaction, the reaction temperature is set at 300˚C, the reaction time is 18 h, and then the white precursor product γ-AlOOH precipitation is generated [17] [18]. After the hydrothermal reaction is completed, the resulting white precursor product is separated by centrifugation and filtration. Then the white precursor product is baked at a temperature of 1100˚C - 1200˚C for 24 h, and the product obtained is the final α-Al_2O_3.

2.3. Modification of Nanometer α-Al_2O_3

The particle size of the nano-α-Al_2O_3 powder particles is small and the specific surface area is large, which indicates that there are more surface atoms or molecules per unit mass or volume that are the active sites where silane coupling agents can bind. Therefore, smaller particle sizes can provide more opportunities to react with silane coupling agents. Secondly, the smaller particle size of the nano-α-Al_2O_3 particles have better dispersion in solution, which helps the silane coupling agent to cover the surface of the particles more evenly, which not only improves the efficiency of the modification, but also helps to improve the stability of the modified material. However, the agglomeration of nano-α-Al_2O_3 powder particles is obvious and it has hydrophilic properties, which makes it difficult to infiltrate in organic solvents and has poor dispersibility. Therefore, in order to stably improve its uniform dispersion, surface modification of nano-α-Al_2O_3 is required before use.

At present, most of the research on the surface organic modification of nanoparticles use surfactants and fatty acids to modify their surface, and the connection methods are mainly through physical adsorption and chemical adsorption. In recent years, the research on the use of silane coupling agents for surface modification has gradually emerged [19] [20] [21].

In this study, silane coupling agent (KH560) was used to modify the surface of nano-α-Al_2O_3 [22] [23] [24] [25] [26]. The group methoxy (Si-OCH_3) in the silane coupling agent reacts with water to form silyl alcohol groups (Si-OH), and then one of the silyl alcohol groups is hydrogen-bonded with the hydroxyl group on the surface of the nano-α-Al_2O_3 to form a -Si-O-Z-covalent bond (Z represents the surface of nano-α-Al_2O_3). The other two silanol groups and silane coupling agent molecules between the silanol group condensation reaction, forming the silicon oxygen chain. The silane coupling agent molecules are cross-linked to form a network structure covering the alumina surface, which has excellent flexibility, adhesion and hydrophobic properties. The reaction mechanism is shown in **Figure 1**.

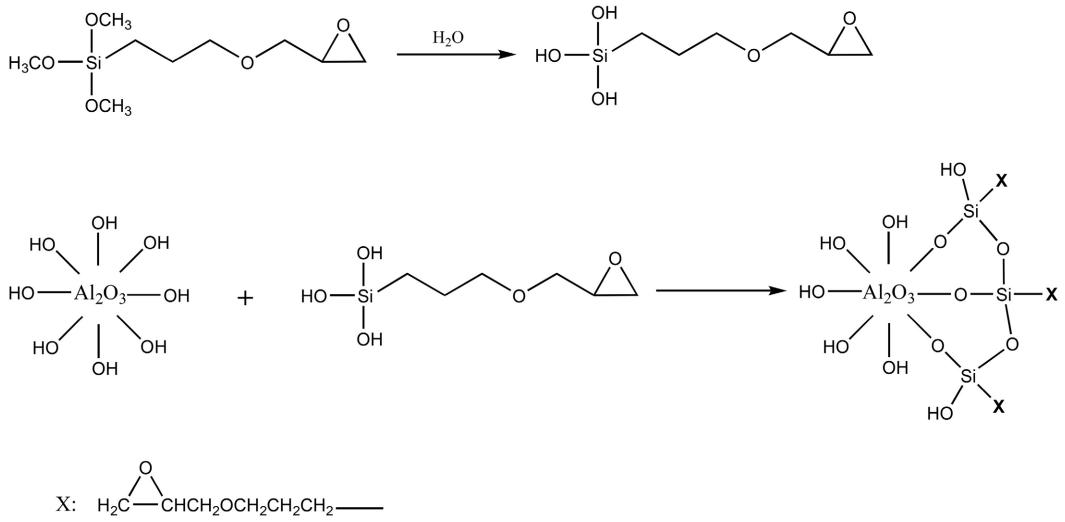

Figure 1. Reaction mechanism of silane coupling agent KH-560 modified nano $A1_2O_3$ particles.

α-Al_2O_3 particles form a good interface combination with polyurethane resin to reduce interface defects and improve the overall performance of the composite. Secondly, α-Al_2O_3 has excellent high temperature stability, which can effectively prevent the thermal decomposition and oxidation of polyurethane resin at high temperatures. This not only extends the service life of the composite, but also enables it to maintain stable performance in extreme temperature environments. At the same time, α-Al_2O_3 particles are used as hard fillers to significantly improve the hardness, wear resistance and impact resistance of polyurethane resin. This allows the composite to better maintain its integrity when subjected to external pressures or shocks, thus providing greater protection.

2.4. Preparation of Passivation Solution

2.4.1. Preparation of Modified Nano-α-$A1_2O_3$ Dispersion Solution

Add 7% mass fraction nano-α-Al_2O_3 powder particles into the three-port flask, add ethanol aqueous solution with a mass ratio of 2:1, mechanically stir for 50 min, add 10% mass fraction of silane coupling agent KH560, and stir continuously, while the pH value of the solution is adjusted to about 7. After continued stirring for 2 - 3 h, the nano-α-Al_2O_3 dispersion liquid was obtained by ultrasonic dispersion for 3h in the ultrasonic oscillator.

2.4.2. Preparation of Passivation Solution

250 ml deionized water, 400 g/L waterborne polyurethane, 8 g/L H_2O_2-modified fluotitanic acid and 40 g/L silane coupling agent KH560 were added into the reaction dish. The prepared nano-α-Al_2O_3 dispersion was added while stirring, and the temperature was controlled at 40˚C - 60˚C for 2 - 3 h by ultrasonic oscillation. The chromium-free passivation solution of modified nano-α-$A1_2O_3$ was obtained.

2.4.3. Passivation Film Coating

The chromium-free passivation solution was evenly coated on the surface of the

substrate with RDS-5 paint rod and was taken out in the oven for 30 seconds and left for 48 h at room temperature.

The experimental group was compared to prepare single waterborne polyurethane coated galvanized sheet and blank galvanized sheet.

2.5. Experiments

2.5.1. Nano-α-$A1_2O_3$ Modification Test

The particle size of nano-α-$A1_2O_3$ after modification was tested by ZS90 nanometer particle size meter produced by Malvern Panalytical in the UK, and its dispersion was analyzed according to its PDI (polymer dispersion index) and average particle size.

The structure of nano-α-$A1_2O_3$ before and after modification was tested by Fourier infrared spectrometer (FTIR) Nicolet 6700 produced by Nicolet, USA [27], and the scanning range was 4000 - 500 cm^{-1}.

2.5.2. Passivation Film Surface Performance Test

By testing the film thickness, film adhesion and surface hardness of single waterborne polyurethane passivation film and nano α-$A1_2O_3$ modified composite polyurethane passivation film, the performance difference between the two is compared, the specific test is as follows:

Weighing method was used to test the thickness of passivation film [28] [29] [30], test the mass of substrate M1 before coating, test the mass of substrate M2 after coating cure, calculate the coating surface area S, and calculate the coating film thickness according to the following calculation Equation (1):

$$\text{Coating film thickness} = \frac{M2 - M1}{S} \tag{1}$$

The adhesion of the coating surface was tested using the adhesion guide gauge, and the test results were rated according to GB/T 9286-2021 "Paint and Varnish grid Test".

The surface hardness of the sample to be tested was measured by digital micro-Vickers hardness tester, and the hardness difference between the two was compared to measure the effect of nano-α-Al_2O_3 on the surface hardness of the substrate.

2.5.3. Electrochemical Testing [31] [32]

CHI660 electrochemical workstation produced by Shanghai Chenhua Company was used for electrochemical test, with three electrode system, galvanized plate working electrode, working area of $1cm^2$, platinum sheet as auxiliary electrode and saturated calomel electrode as reference electrode. The experimental temperature was 20˚C - 25˚C, and the corrosive medium was 3.5% NaCl solution. The scanning range of Tafel polarization curve is −1.5 - −0.5 V, and the scanning rate is 1 mV/s. The AC impedance test frequency is set to 10^{-2} - 10^5 Hz, and the amplitude of the disturbance signal is 5 mV. origin was used for Tafel data fitting, and the impedance data were fitted by Z-simpwin software and Z-view software.

2.5.4. Neutral Salt Spray Test

This test was carried out according to the national standard GB 6458-86 "Neutral salt spray test on Metal Covering Layer", the base material size was 80 mm × 150 mm (working area was 70 mm × 140 mm), the mass fraction of NaCl solution was 3.5%, the pH of the solution was controlled between 6.5 - 7.5, and the temperature in the salt spray chamber was controlled at 32˚C - 36˚C. The salt spray settlement was controlled at 0.0135 - 0.0235 mL/(cm²·h), and the experimental sample was formed at 35˚ - 45˚ perpendicular to the support in the box. After continuous spraying for 72 h, the sample was cleaned and weighed, and the corrosion resistance of the sample was determined by calculating the proportion of the surface area of white rust [33].

2.5.5. Surface Microtopography

Nissan JSM-6490LV scanning electron microscope (SEM) was used to observe the surface micro-morphology of galvanized blank plate, single water-based polyurethane passivation film and nano α-Al_2O_3 modified composite polyurethane passivation film [34], and compare the morphological differences among the three, with an acceleration voltage of 20 kV.

3. Results and Discussion

3.1. Modification Effect of Nano-α-$A1_2O_3$

3.1.1. Particle Size Measurement

According to the previous experimental description, the experimental scheme design is shown in **Table 1**. In **Table 1**, nine kinds of modified nano-α-Al_2O_3 dispersions were tested. After ultrasound, they were left for a period, and their particle sizes were measured at room temperature (20˚C - 25˚C) using ZS90 nano-particle size potential analyzer produced by Malvern Panalytical Company in the UK. The results are shown in **Figure 1**.

Table 1. Micro-nano α-Al_2O_3 modification test scheme.

Number	Factor A	Factor B		Factor C
	Dosage of nano-α-Al_2O_3/g	Water:Ethanol (m:m)	Ethanol aqueous solution/ml	KH560 hydrolysate/g
1	0.03	1:1	9.94	0.03
2	0.03	1:2	9.92	0.05
3	0.03	1:3	9.9	0.07
4	0.05	1:1	9.9	0.05
5	0.05	1:2	9.88	0.07
6	0.05	1:3	9.92	0.03
7	0.07	1:1	9.86	0.07
8	0.07	1:2	9.9	0.03
9	0.07	1:3	9.88	0.05

The particle size PDI (polymer dispersion index) values of the 9 samples measured in Figure 2 are all within 0 - 0.5. As can be seen from Figure 2, sample No. 5 has the smallest particle size, with an average particle size of 222.7 nm. At the same time, according to the above particle size distribution diagram, it can be seen that different nano-α-Al_2O_3 content, different ethanol aqueous solution ratio, and different silane coupling agent ratio have certain effects on particle size distribution. With the increase of nano-α-Al_2O_3 content, its particle size gradually decreases, but with the increase of its content, the particle size also significantly increases, and in the subsequent experiment, it is found that when the content exceeds a certain amount, the PDI of the measured data will stabilize at 1, indicating that the test data at this time has a huge deviation. At the same time, when the ratio of ethanol solution is (2 or 3):1, and the dosage of silane coupling agent is 5% - 7%, the dispersion of nano-α-Al_2O_3 with 5% mass fraction is the best.

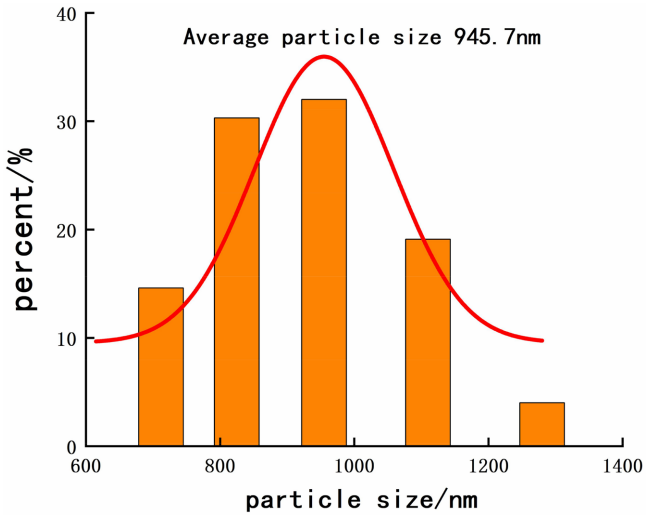

(a)

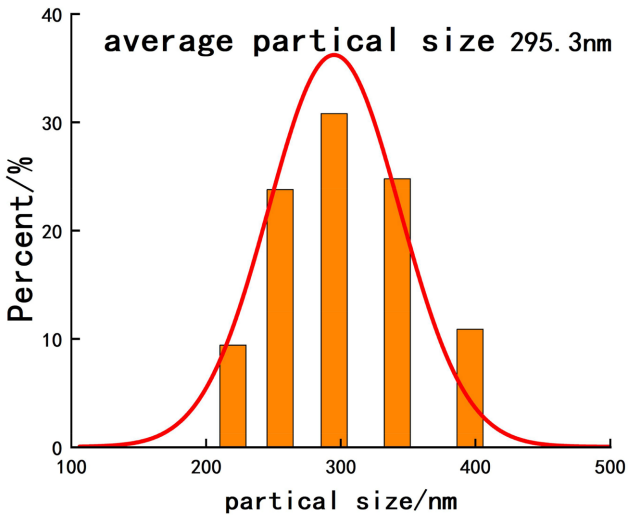

(b)

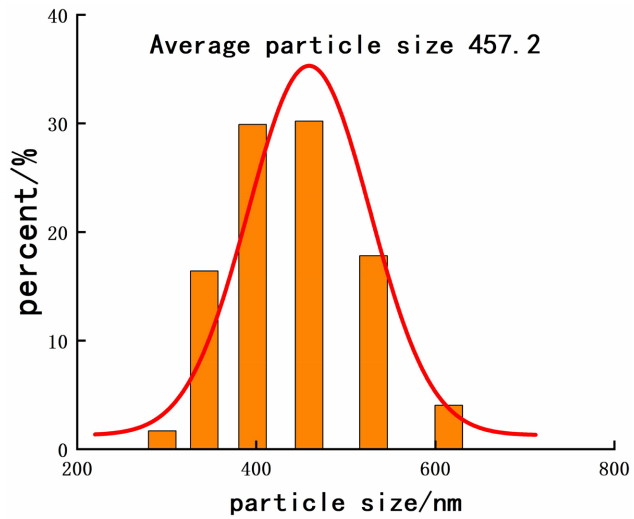

(c)

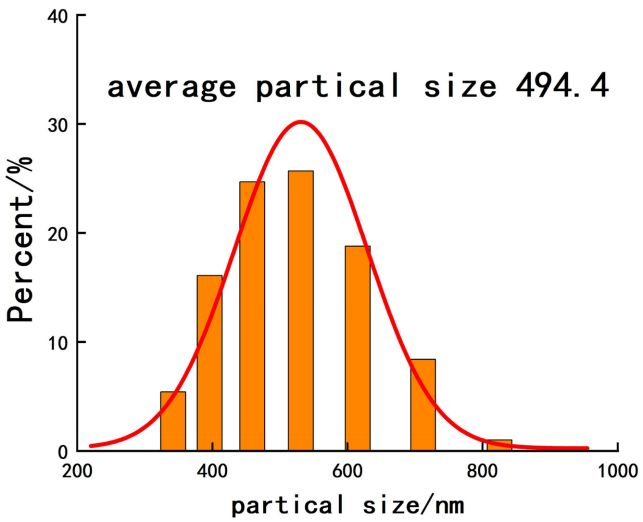

(d)

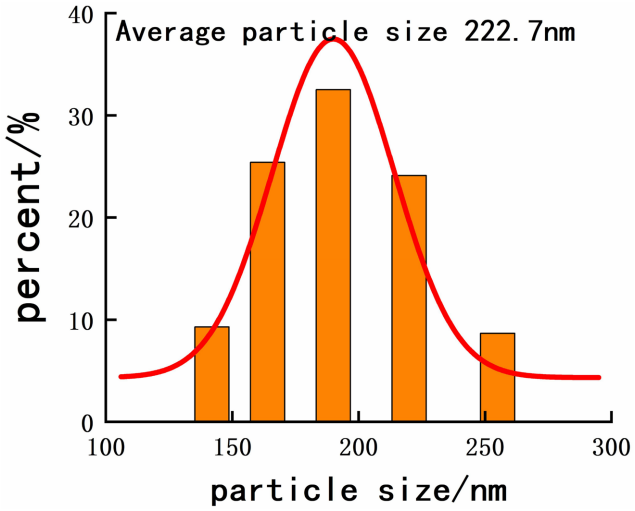

(e)

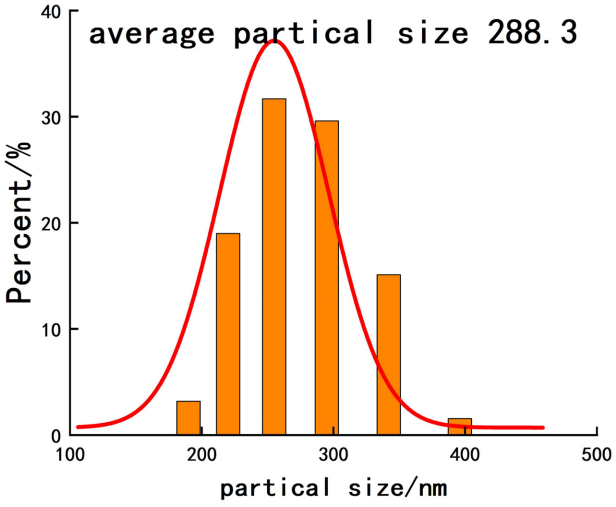

(f)

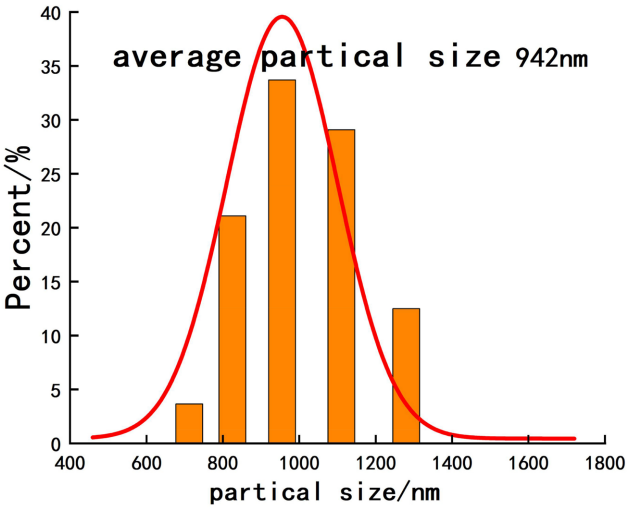

(g)

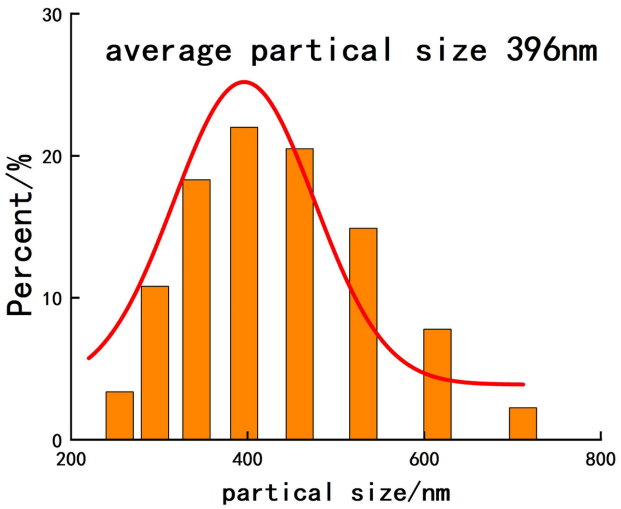

(h)

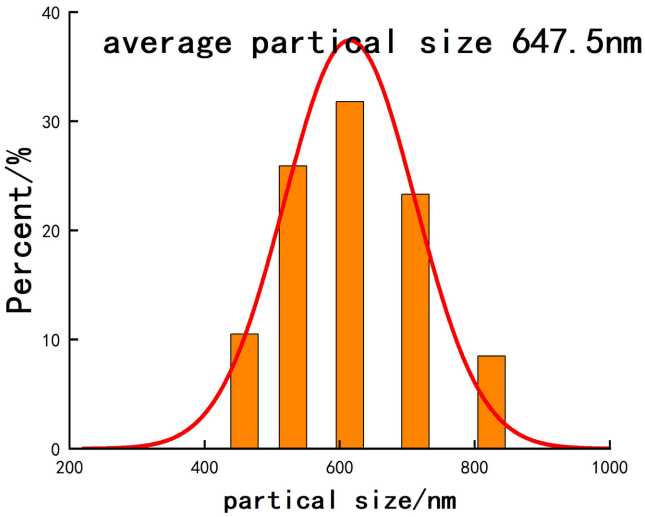

(i)

Figure 2. Particle size distribution of modified micro-nano α-Al_2O_3.

3.1.2. Fourier Infrared Test

Figure 3 shows the Fourier infrared spectra of nano-α-Al_2O_3 before and after modification, and Figure 3(a) and Figure 3(b) show the FTIR spectra before and after modification, respectively. It can be seen from Figure 2 that before and after modification of nano-α-Al_2O_3, 3440 cm^{-1} and 1630 cm^{-1} are the stretching vibration peaks and vibration absorption peaks of O-H and H-OH. There is a certain wide absorption band in the range of 500 - 1000 cm^{-1}, which is the characteristic absorption peak of nano-Al_2O_3, indicating that the internal structure of nano-α-Al_2O_3 is not damaged after modification. After modification, different vibration peaks were observed in the spectrum: methyl asymmetric stretching vibration peak at 2940 cm^{-1}, methylene symmetric stretching vibration peak at 2840 cm^{-1}; the absorption peak of 1466 cm^{-1} corresponds to the bending vibration of C-H bond. The absorption peak of epoxy-group stretching vibration is at 1200 cm^{-1}, and the asymmetric stretching vibration peak of Si-O-Si bond is at 1080 cm^{-1}. It can be seen from the above that the modified trimethylchlorosilane has been successfully connected to the surface of nanometer α-Al_2O_3.

3.2. Passivation Film Surface Performance Test

3.2.1. Film Thickness of Passivation Film

The passivation film formed by coating only a single water-based polyurethane passivation solution and nano-α-Al_2O_3 modified composite polyurethane passivation solution was selected. The data of 20 sample points were uniformly selected on the substrate of the film layer, and the mean value and standard deviation were calculated to represent the film thickness to facilitate the reduction of errors. The test results were shown in Figure 4.

The average film thickness of single waterborne polyurethane passivation film was 1.653 g/m^2, and the film thickness of nano α-Al_2O_3 modified polyurethane composite passivation film was 1.722 g/m^2.

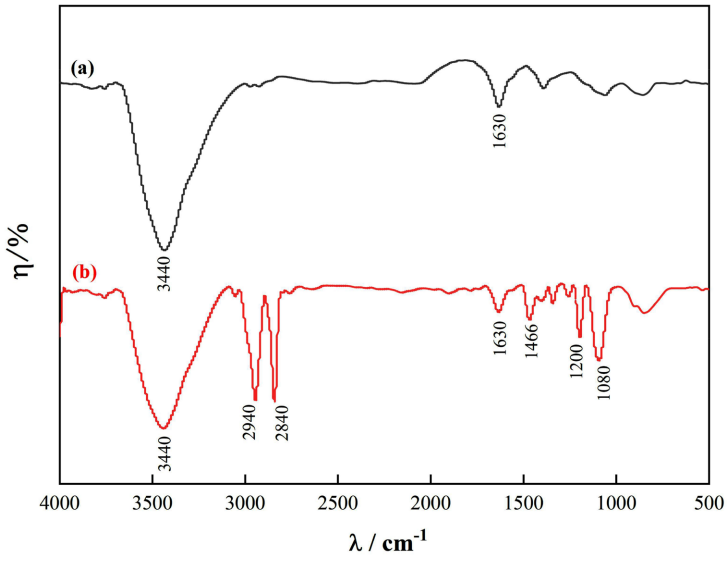

Figure 3. Infrared spectra before and after modification of micro-nano α-Al_2O_3.

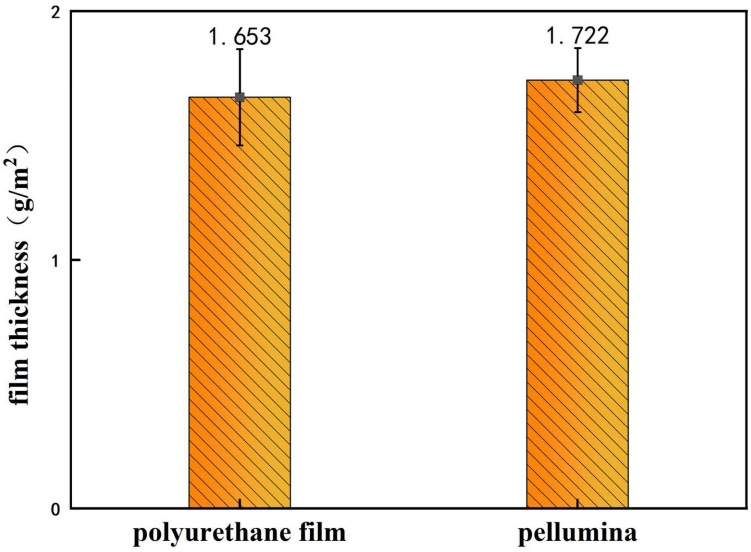

Figure 4. Film thickness of passivation film.

3.2.2. Surface Adhesion

The substrate surface adhesion test equipment is a guide gauge tester, so that the bottom surface of the guide gauge is flat with the object to be measured. The cutting speed of LC-302 manual knife is 25 - 35 mm/S, and the cutting incision should obviously pass through the coating and not cut into the substrate too deeply. After cutting 6 marks, rotate 90˚ and repeat the previous cutting operation. Observe the coating cutting area and determine the adhesion level according to the GB/T 9286-2021 "Paint and varnish·grid Test" rating standard.

The test results are shown in **Figure 5**. 1-1# and 1-2# are the single water-based polyurethane passivation film and the nano-α-Al_2O_3 modified composite polyurethane passivation film, respectively. The surface marks are smooth around the scratch, and no debris falls off around the scratch. Both passivation films have excellent adhesion on the surface of the measured galvanized sheet.

3.2.3. Surface Hardness Test

The surface hardness test results of the samples (galvanized steel sheet) are shown in **Figure 6**. Fifteen test points were uniformly selected on the surface of each sample for hardness measurement. To minimize errors, the highest and lowest values were excluded, and the average measurement value of the remaining points was taken to represent the hardness value of the sample. As indicated in **Figure 6**, there was little difference in hardness values between the blank galvanized plate and the single-component waterborne polyurethane galvanized plate. This suggests that waterborne polyurethane resin does not possess the capability to enhance the substrate hardness. This is attributed to the main components of the passivation solution, which include waterborne polyurethane resin, silane coupling agent, and inorganic components. These substances primarily serve to enhance corrosion resistance and adhesion, rather than increasing surface hardness.

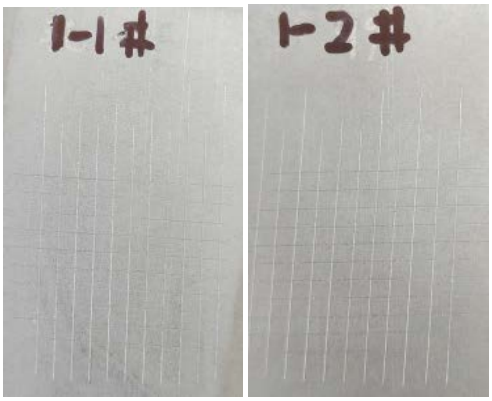

Figure 5. Adhesion test of passivation film.

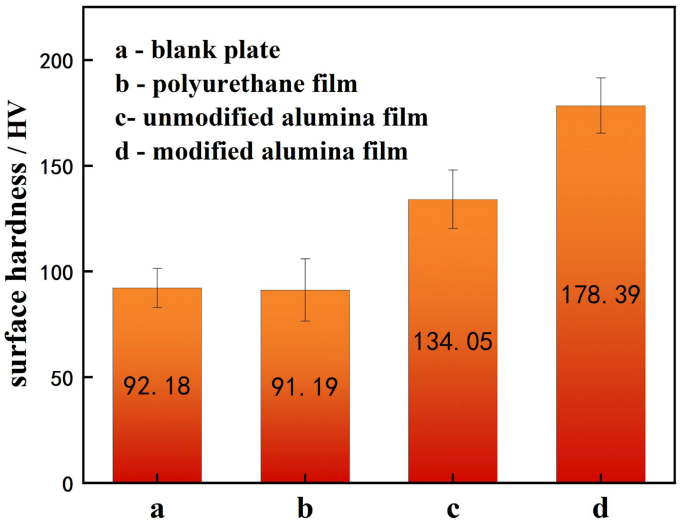

Figure 6. Surface hardness of the film.

Both unmodified nano α-Al_2O_3 and modified nano α-Al_2O_3 polyurethane resin coatings increased the surface hardness of galvanized steel sheet. This enhancement was attributed to the excellent hardness, mechanical strength, and abrasion resistance inherent in nano α-Al_2O_3. However, compared to the unmodified nano α-Al_2O_3 film, the improvement in surface hardness was more pronounced with the modified nano α-Al_2O_3 polyurethane resin coating. In comparison to the blank galvanized plate, the hardness values increased by 47% and 85%, respectively, for the two coatings. This indicates that the effect of modified nano α-Al_2O_3 was more significant.

3.3. Passivated Film Resistance to Electrochemical Corrosion Test

3.3.1. Tafel Polarization Curve

The Tafel polarization curve test results for the blank galvanized sheet, waterborne polyurethane-coated galvanized sheet, and modified nanoscale α-Al_2O_3 composite polyurethane-coated galvanized sheet are shown in Figure 7, with the parameters of the test results provided in Table 2. From Table 2, it can be observed that the corrosion current gradually decreases from the blank galvanized

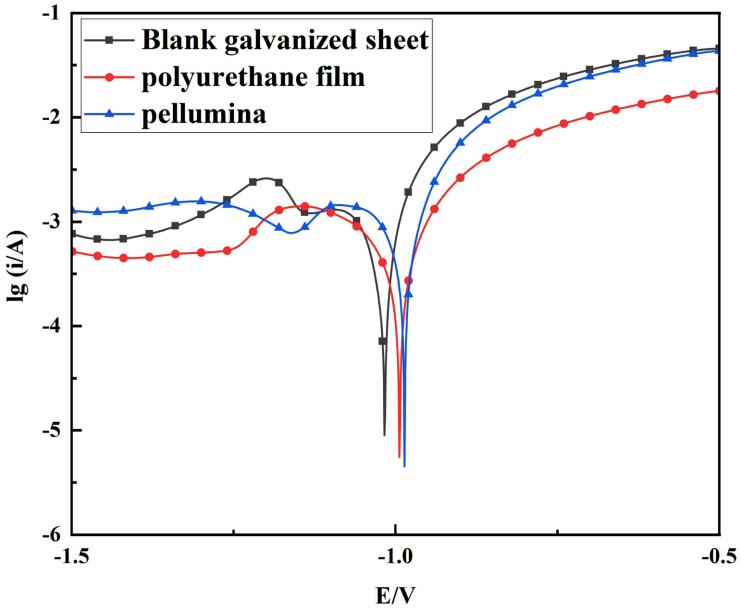

Figure 7. Tafel polarization curves of the three samples.

Table 2. Electrochemical parameters of Tafel polarization curves of three samples.

samples	E_{corr}/V	J_{corr}/(A·cm^{-2})	R/(Ω·cm^2)
Blank sheet	−1.012	8.47×10^{-4}	65.3
polyurethane film	−1.006	3.91×10^{-4}	140.1
pellumina	−1.014	2.05×10^{-4}	232.3

sheet to the aluminum oxide film-coated galvanized sheet, indicating that both cathodic and anodic reactions within the reaction vessel are gradually inhibited, resulting in a reduction in the rate of electron transfer and making corrosion reactions within the solution easier to suppress. This indicates that the corrosion rate of the corrosion medium to the plate is gradually reduced, and the corrosion resistance of the plate is improved. Simultaneously, the polarization resistance gradually increased and increased significantly. The polarization resistance of the waterborne polyurethane film was 140.1 Ω·cm^2, about 2.5 times that of the blank galvanized sheet, and the polarization resistance of the alumina film was 232.3 Ω·cm^2, 4 times that of the blank galvanized sheet. This indicates that the corrosion resistance of alumina film to corrosive media is more prominent than that of waterborne polyurethane film, and the protection effect on the surface of galvanized sheet is better.

3.3.2. Impedance Test

The results of the electrochemical impedance spectroscopy (EIS) tests are illustrated in **Figure 8** and **Figure 9**. **Figure 8** displays the Nyquist plots for the three test samples, along with the equivalent circuit diagrams used during fitting, while **Figure 9** depicts the Bode plots for the three samples.

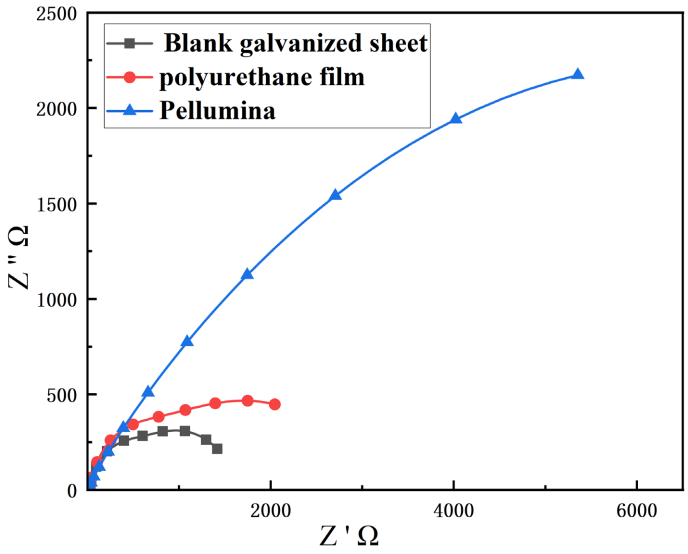

Figure 8. Nyquist spectrum of AC impedance.

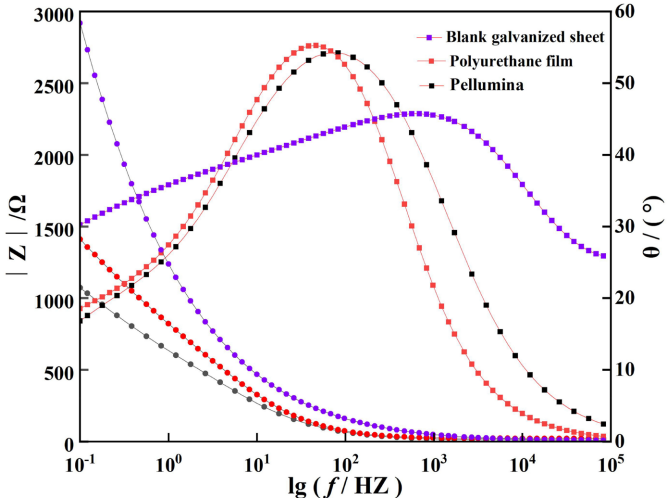

Figure 9. Bode diagram of AC impedance.

From Figure 8, it can be observed that the small semicircles in the first half correspond to the high-frequency region, with the radius of the semicircle for the aluminum oxide film being much larger than that of the blank sheet and polyurethane film. This indicates that the electron transfer rate on the surface of the aluminum oxide film is slow, and it exhibits strong inhibition of charge reactions within the solution. In the second half, representing the low-frequency region, the capacitive arc of the waterborne polyurethane film is slightly larger than that of the blank galvanized sheet, while the capacitive arc of the aluminum oxide film is much larger than both the blank sheet and polyurethane film. This suggests that the aluminum oxide film exhibits strong resistance to the corrosive medium within the solution and is more effective in inhibiting corrosion reactions.

According to Figure 9, the magnitude of impedance (|Z|) for the aluminum oxide film at low frequencies is significantly larger than that for the blank sheet

and the polyurethane film. In the mid-frequency region, peaks appear for the blank sheet and polyurethane film, while the peak for the aluminum oxide film occurs in the high-frequency region. The phase angle of the aluminum oxide film in the high-frequency region is significantly higher than that of the blank sheet and polyurethane film, indicating that the aluminum oxide film exhibits stronger inhibition of corrosion reactions within the solution and is more effective in preventing penetration by the corrosive medium. This observation aligns with the results reflected by the capacitive arcs in the Nyquist plot.

Table 3 shows the parameter values of the impedance fitting equivalent circuit. Compared with blank galvanized sheet and single waterborne polyurethane film, the impedance value of the nano-α-Al_2O_3 film shows an obvious trend of increase. The content of Nyquist diagram and Bode diagram is intuitively presented from the data. This is because after the nano α-Al_2O_3 modified waterborne polyurethane composite coating, the density of the film layer is better than that of a single polyurethane film. At the same time, nano-α-Al_2O_3 gives the film layer more excellent corrosion resistance, which is more conducive to the inhibition of corrosive media, so the corrosion resistance will be better.

3.4. Neutral Salt Spray Test

The results of the neutral salt spray corrosion test on the passivation films are depicted in Figure 10, where Figures 10(a)-(c) correspond to the blank galvanized sheet, single waterborne polyurethane-coated galvanized sheet, and modified nanoscale α-Al_2O_3 composite polyurethane passivated galvanized sheet, respectively. From Figure 11(a), it can be observed that the surface of the galvanized sheet is covered with white and yellow rust. The white rust is a white precipitate of Zn $(OH)_2$ formed after the surface zinc elements of the galvanized sheet corroded. Subsequently, yellow rust appeared, indicating that the galvanized layer had been corroded by saltwater penetration, directly corroding the steel plate surface to form rust, with corrosion area approaching 100%, indicating relatively weak corrosion resistance of the blank galvanized sheet. The corrosion area in Figure 11(b) is 40%, with complete corrosion around the galvanized sheet and deeper corrosion. There are also small areas of white rust corrosion in the middle. The corrosion area in Figure 11(c) is 10%, with corrosion occurring around the periphery but with shallow corrosion depth, and no corrosion in the middle. The surface of the blank zinc plate is not coated with passivation liquid, so that its resistance to corrosive medium is weak, the corrosive medium can quickly corrosion through the galvanized plate, and then corrosion inside the steel plate, water-based polyurethane has a certain defense ability to the corrosive medium, which makes the corrosive medium penetrate the zinc layer very slowly, but also causes corrosion to the zinc layer to a certain extent. The nano-α-Al_2O_3 composite polyurethane film has strong resistance to corrosive media, which makes the corrosion rate of corrosive media very low, and also makes it difficult to corrode the inside of the plate. This indicates that the corrosion resistance of the blank galvanized sheet is relatively weak. The corrosion resistance

of the single waterborne polyurethane-coated galvanized sheet is significantly improved compared to the blank galvanized sheet. However, the modified nanoscale α-Al_2O_3 composite polyurethane passivated galvanized sheet exhibits excellent corrosion resistance, far surpassing that of the single waterborne polyurethane-coated galvanized sheet.

Table 3. Parameter values of impedance fitting equivalent circuit.

Sample	R_1/ ($\Omega \cdot cm^2$)	C_1 ($F \cdot cm^2$)	R_2 ($\Omega \cdot cm^2$)	C_2 ($F \cdot cm^2$)	R_3 ($\Omega \cdot cm^2$)
Blank sheet	9.49	1.37×10^{-4}	552.5	1.10×10^{-3}	1079
polyurethane film	20.95	8.11×10^{-5}	609.7	8.96×10^{-4}	2645
pellumina	53.66	3.61×10^{-5}	1653.4	2.43×10^{-4}	5939

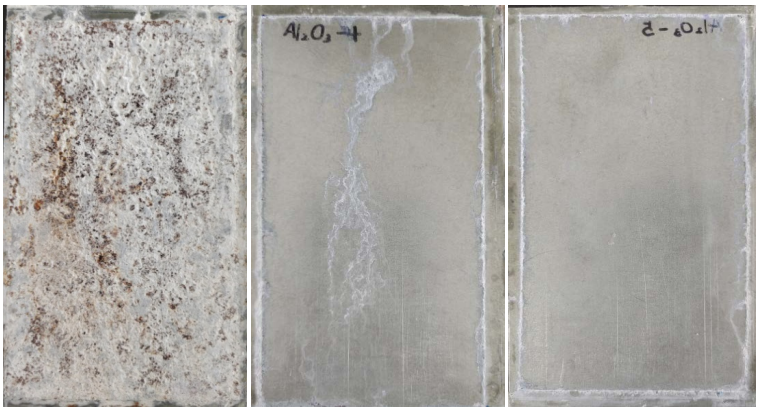

(a) (b) (c)

Figure 10. Results of neutral salt spray test.

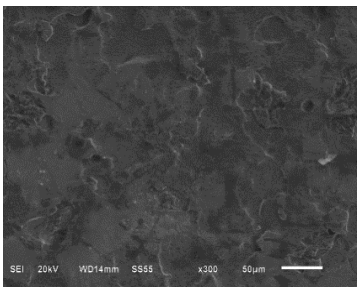

(a)

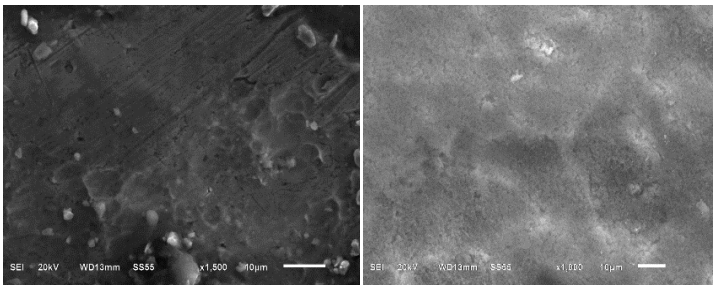

(b) (c)

Figure 11. SEM images of three samples.

3.5. Analysis of Surface Morphology of Passivation Film

The scanning electron microscopy (SEM) test results are shown in **Figure 11**, where **Figures 11(a)-(c)** correspond to the surface microstructures of the blank galvanized sheet, waterborne polyurethane film on the galvanized sheet surface, and modified α-Al_2O_3 polyurethane film, respectively. **Figure 11(a)** depicts SEM images magnified at 300 times, showing numerous depressions, pores, and some noticeable cracks on the surface. **Figure 11(b)**, when magnified at 300 times, exhibits no obvious depressions, but upon further magnification to 1500 times, surface grooves and pores are still present, indicating that although the polyurethane film partially improves the surface properties of the blank galvanized sheet, some defects persist. In **Figure 11(c)**, at 1500 times magnification, no obvious cracks or pores are observed, and a relatively dense structure is formed, effectively compensating for the defects in the polyurethane film of **Figure 11(b)**. This suggests that the modified nano α-Al_2O_3 particles adequately fill the existing pores and cracks on the surface. Additionally, a mesh-like structure is formed on the film surface, which is a planar structure of the film formed by the cross-linking polymerization of polyurethane, silane coupling agent, modified nano α-Al_2O_3 particles, and other substances in the passivation solution. The mechanical strength of this film is more stable than that of the galvanized sheet film in **Figure 11(a)** and **Figure 11(b)**, resulting in better chemical resistance.

4. Conclusions

The nanoscale α-Al_2O_3 particles exhibited significant aggregation and were difficult to disperse due to their small size. Surface modification of the nanoparticles with the silane coupling agent KH560 was performed, resulting in a significant reduction in particle size when dispersed in the solution. Furthermore, the influence of the proportion of ethanol-water solution and the dosage of the silane coupling agent KH560 on the dispersibility of the nanoscale α-Al_2O_3 particles was investigated. The experimental results indicated that a ratio of 2:1 for ethanol-water and a KH560 dosage of 5% showed the best dispersing effect.

According to the surface hardness test results of the galvanized sheet, a single waterborne polyurethane resin coating did not enhance the surface hardness of the galvanized sheet. However, after introducing modified nanoscale α-Al_2O_3, the surface hardness of the galvanized sheet was significantly increased, showing an 85% improvement over the original hardness. Furthermore, the electrochemical corrosion resistance test results showed that the corrosion resistance of the modified nanoscale α-Al_2O_3 polyurethane resin composite coating was superior. While a single polyurethane film exhibited better corrosion resistance compared to the blank galvanized sheet, the corrosion resistance of the nanoscale α-Al_2O_3 film was even more remarkable than that of the single polyurethane film. Moreover, based on the scanning electron microscopy test results, it was observed that the modified nanoscale α-Al_2O_3 polyurethane resin composite coating formed a smooth and dense film layer on the surface of the galvanized sheet, effectively

compensating for surface defects such as grooves and holes. This improvement is expected to significantly enhance the surface performance of the galvanized sheet.

Authors' Contributions

Conceptualization, L.X.W. and Q.F.Z.; methodology, L.X.W. and Y.Z.; software, L.X.W and Y.Z..; validation, Q.F.Z., Y.Z. and X.Z.G; formal analysis, L.X.W.; investigation, Y.Z..; writing—original draft preparation, L.X.W.; writing—review and editing, Y.J. and Q.F.Z.; visualization, L.X.W; supervision, Q.F.Z.; project administration, Q.F.Z.; funding acquisition, Y.J. All authors have read and agreed to the published version of the manuscript.

Data Availability

The data used and/or analyzed during the current study are available from the corresponding author on reasonable request.

Acknowledgements

The paper was partially supported by National Natural Science Foundation of China (42271301), Anhui University Excellent Research and Innovation Project (No. 2022AH010094). Authors appreciate the reviewers for their invaluable comments which have led to significant improvement in the paper.

Conflicts of Interest

The authors declare no conflicts of interest regarding the publication of this paper.

References

[1] Fu, Q.L., Wu, A.R., Du, W.H., *et al.* (2020) Application Status and Prospect of Surface Strengthening Technology for Metal Materials. *Journal of Hunan Institute of Engineering*, **30**, 52-56.

[2] Wu, H.J., Chen, J.H. and Lu, J.T. (2004) Research Progress on Corrosion Resistance Mechanism of Zinc Plating Without Chromium Passivation. *Material Protection*, **37**, 43-45.

[3] Wang, L. (2012) Preparation, Properties and Film-Forming Mechanism of Silane Composite Passivation Film on Galvanized Sheet Surface. Ph.D. Thesis, Thesis, Northeastern University, Shenyang.

[4] Zhao, X.F., Yang, R.F., Miao, Y.F., *et al.* (2014) Study on Microstructure and Electrochemical Properties of Zn-Zr Composite Nanofilms on Hot Galvanized Sheet Surface. *Corrosion Science and Protection Technology*, **26**, 459-463.

[5] Nie, D.W. (2019) Preparation and Properties of Hydrophilic Resin on Galvanized Sheet Surface. Ph.D. Thesis, Dalian Polytechnic University, Dalian.

[6] Wu, H.B., Xu, B. and Tan, Z.Q. (2019) Research Progress of Chromium-Free Passivation Process for Metal Surface. *Guangzhou Chemical Industry*, **47**, 31-32, 79.

[7] Fedel, M., Druart, M.E., Olivier, M., *et al.* (2010) Compatibility between Catapho-

retic Electro-Coating and Silane Surface Layer for the Corrosion Protection of Galvanized Steel. *Progress in Organic Coatings*, **69**, 118-125. https://doi.org/10.1016/j.porgcoat.2010.04.003

[8] Hou, K.W., Li, Y.X., Zhou, J.P., *et al.* (2020) Preparation and Coating Properties of Cationic Photocurable Waterborne Polyurethane. *Journal of Nanchang Hangkong University* (*Natural Science Edition*), **34**, 23-29.

[9] Somisetti, V., Narayan, R. and Kothapalli, R.V.S.N. (2019) Multifunctional Polyurethane Coatings Derived from Phosphate Cardanol and Undecylenic Acid Based Polyols. *Progress in Organic Coatings*, **134**, 91-102. https://doi.org/10.1016/j.porgcoat.2019.04.077

[10] Hou, X.Y., Huang, H.B., Li, Y.F., *et al.* (2022) Stability and Variability—*α*-Alumina: From Properties, Synthesis and Application. *China Ceramic Industry*, **29**, 30-38.

[11] Wang, L.P., Guo, Z.H., Chi, J.Z., *et al.* (2015) Research Progress of Multi-Purpose Development of Alumina. *Inorganic Salt Industry*, **47**, 11-15, 62.

[12] Fu, L., Huang, A., Gu, H., *et al.* (2018) Properties and Microstructures of Lightweight Alumina Containing Different Types of Nano-Alumina. *Ceramics International*, **44**, 17885-17894.

[13] Liu, L.Z., Gao, L., Song, Y.X., *et al.* (2008) Effect of Coupling Agent on Structure and Properties of Polyimide/Nano-Al2O3 Hybrid Films. *Journal of Functional Materials*, **39**, 1887-1889.

[14] Wang, Y., Zhu, S.G. and Dong, W.W. (2015) Preparation of Nano-Sized Flake Alumina by Hydrothermal Method. *Journal of Materials Science and Engineering*, **33**, 401-404.

[15] Sun, J.H., Yi, J.F., Qing, P.L., *et al.* (2021) Preparation of Ultrafine Spherical Alumina Powder by Hydrothermal Method. *China Ceramics*, **57**, 30-35.

[16] Ghanizadeh, S., Bao, X., Vaidhyanathan, B., *et al.* (2014) Synthesis of Nano *α*-Alumina Powders Using Hydrothermal and Precipitation Routes: A Comparative Study. *Ceramics International*, **40**, 1311-1319. https://doi.org/10.1016/j.ceramint.2013.07.011

[17] Shin, D.C., Park, S.S., Kim, J.H., *et al.* (2014) Study on *α*-Alumina Precursors Prepared Using Different Ammonium Salt Precipitants. *Journal of Industrial & Engineering Chemistry*, **20**, 1269-1275. https://doi.org/10.1016/j.jiec.2013.07.003

[18] Liao, H., Liao, Q.L. and Wang, F. (2010) Hydrothermal Synthesis of *α*-Alumina Hollow Microspheres. *China Powder Technology*, **16**, 14-17.

[19] Shan, F.R., Yu, Z.M., Luo, L.S., *et al.* (2013) Study on the Surface Modification of Nano-Al2O3 with Silane Coupling Agent KH550. *New Chemical Materials*, **41**, 169-170, 185.

[20] Yao, H.W., Chen, W., Mei, W.T., *et al.* (2023) Effect of Silane Coupling Agent on Aluminum Hydroxide Crushing and Surface Modification. *Light Metals*, *No. 8*, 8-13.

[21] Liu, H.Y., Li, D.L. and Li, X. (2011) Silane Coupling Agent KH-560 Modified Nano-Silica. *Chemical World*, **52**, 456-458, 462.

[22] Wang, H.P., Gui, P.C. and Hu, S.Q. (2020) Comprehensive Experiment on Hydrophobic Modification of Nano-Alumina by Silane Coupling Agent. *Experimental Technology and Management*, **37**, 154-157.

[23] Hao, J. (2023) Study on the Application of Silane Coupling Agent in Nanomaterial Modified Waterborne Polyurethane. *Shanxi Chemical Industry*, **43**, 29-31.

[24] Cao, J., Zhang, Y.X., Wang, X.Z., *et al.* (2016) Exploration of the Conditions for the Modification of Nano-Alumina by Silane Coupling Agent. *New Chemical Materials*, **44**, 207-209.

[25] Chen, J.H. and Zhu, C.L. (2011) Study on the Modification of Nano-Al2O3 with Silane Coupling Agent. *Guangdong Chemical Industry*, **38**, 253-255, 246.

[26] Wang, B., Liu, W., Zhu, Y., *et al.* (2007) A General Procedure for Surface Modification of Nano-Alumina and Its Application to Dendrimers. *Journal of Wuhan University of Technology-Mater. Sci. Ed.*, **22**, 453-456. https://doi.org/10.1007/s11595-006-3453-z

[27] Zhao, C.F., Yi, Z.Y. and Li, B. (2007) Effect of Microstructure of α-Type Alumina on Infrared Spectra. *Spectrum Laboratory*, No. 3, 341-344.

[28] Wu, Z.J. (2022) Gravimetric Determination of Chromium-Free Passivation Film Quality of Galvanized Steel Plate. *Chinese Society of Metals. Proceedings of the* 13*th China Iron and Steel Annual Meeting—Surface and Coating. Inspection and Testing Center of Ben Steel Sheet*, Chongqing, 23 November 2022, 104-107.

[29] Fan, Z.G. (2011) Determination of Coating Quality of Galvanized Steel Plate by X-Ray Fluorescence Spectrometry. *Physicochemical Inspection* (*Chemistry Branch*), **47**, 511-513, 516.

[30] Jiao, Z.H., Feng, Q.Y., Fan, Z.Y., *et al.* (2022) Application of Chromium-Free Passivation Film Thickness Measurement by X-Ray Fluorescence Spectrometry in Galvanizing Units. *Henan Metallurgy*, **30**, 40-43.

[31] Dong, N.N., He, D.J., Liu, W.H., *et al.* (2023) Corrosion Resistance of Chromium-Free Passivated Galvanized Sheet after Forming. *Electroplating and Finishing*, **42**, 56-62.

[32] Xi, P., Yao, Y.H. and Wang, W.F. (2022) Study on Chromium-Free Passivation of Galvanized Sheet Composite and Its Properties. *New Materials for High Speed Railway*, **1**, 36-40.

[33] Kang, Y.F. (2020) Study on Corrosion Resistance of Chromium-Free Passivation Film of Hot-Dip Galvanized Steel Sheet. *Shandong Metallurgy*, **42**, 37-39.

[34] Zheng, X.R., Liu, C., Yu, X.H., *et al.* (2018) Microstructure and Corrosion Resistance of Chromium-Free Composite Passivation Films. *Surface Technology*, **47**, 197-203.